Available online at www.sciencedirect.com
ScienceDirect
Surface Science 600 (2006) 4305–4309
SURFACE SCIENCE
www.elsevier.com/locate/susc

Structural, electronic and magnetic properties of vacancies in single-walled carbon nanotubes

W. Orellana *, P. Fuentealba

Departamento de Física, Facultad de Ciencias, Universidad de Chile, Casilla 653, Santiago, Chile

Available online 22 May 2006

Abstract

The monovacancy and the divacancy in single-walled carbon nanotubes (CNTs) are addressed by spin-density functional calculations. We study these defects in four nanotubes, the armchair (6,6) and (8,8) and the zigzag (10,0) and (14,0), which have diameters of about 8 and 11 Å, respectively. We also consider different defect concentrations along the tube axis. Our results show that CNTs with a monovacancy exhibit ferromagnetism with magnetic moments ranging from 0.3 to 0.8 μ_B. Whereas, CNTs with a divacancy do not exhibit magnetism due to the full reconstruction around the defect where all C atoms are three fold coordinated. We observe that the monovacancy does not change drastically the CNT electronic properties, preserving their corresponding metallic or semiconducting character. However, both armchair and zigzag CNTs with a divacancy become small-gap semiconductors with an energy gap of about 0.15 eV.

Keywords: Carbon nanotubes; Vacancies; Magnetic surfaces; Density functional calculations

1. Introduction

The study of defects in carbon nanostructures have become considerably important since the recent experimental findings of magnetic ordering in pressure-induced polymerized fullerenes [1,2] and proton-irradiated graphite which exclude metal impurities [3]. Magnetism in defective graphite have been also predicted theoretically [4]. However, experimental evidence of defect-induced magnetism in CNT samples is still lacking due to the presence of metal catalysts. Calculations on open ended zigzag nanotubes are found to exhibit energetically favorable ferromagnetic ordering which are associated to unsaturated dangling bonds at zigzag edges [5]. Single vacancies in CNTs with small diameters, ranging from 4 to 8 Å, have been recently addressed by first-principles calculations [7]. Although relative high concentrations of vacancies or small supercell sizes containing a vacancy have been considered in this work, it shows that only metallic nanotubes with a single vacancy in their ground state equilibrium geometries would exhibit ferromagnetism.

2. Theoretical approach

The calculations were performed in the framework of the spin-polarized density functional theory, using a basis set of numerical pseudoatomic orbitals as implemented in the code SIESTA [8]. The exchange-correlation energy is calculated within the generalized gradient approximation [9]. Standard norm-conserving pseudopotentials in their separable form are used to describe the electron-ion interaction. We use a double-ζ singly-polarized basis set. We study the vacancies in both armchair and zigzag CNTs with different sizes. The armchair CNTs have chiral indices of (6,6) and (8,8), and the zigzag ones (10,0) and (14,0). These tubes have diameters of about 8 and 11 Å, respectively [6]. The armchair and zigzag CNTs were described using supercell with lengths of $L_1 = 12.46$ Å and $L_2 = 12.96$ Å, respectively, where periodic boundary conditions are applied only along the tubes axis. This means that we are calculating CNTs with a linear density of defects. For the Brillouin zone sampling we use six k points along the

* Corresponding author.
E-mail address: worellana@macul.ciencias.uchile.cl (W. Orellana).

0039-6028/$ - see front matter © 2006 Elsevier B.V. All rights reserved.
doi:10.1016/j.susc.2006.01.158

CNT axis [10]. To ensure negligible interaction between tubes we imposed a vacuum region of 12 Å. Longer supercells with lengths up to $2L$ are also considered to study the effect of a lower defect concentrations in (6,6) and (10,0) CNTs, which were described with supercells containing up to 240 atoms and the Γ point for the BZ sampling. The positions of all atoms were relaxed using the conjugated gradient algorithm until the force components become smaller than 0.05 eV/Å.

3. The monovacancy in carbon nanotubes

Fig. 1(a) and (b) shows respectively the equilibrium geometries of the (6,6) and (10,0) CNTs containing the monovacancy (hereafter referred to as (6,6) + 1 V and (10,0) + 1 V). We find that the neighboring C atoms partially reconstruct around the defect, forming a pentagon bonding structure, leaving a C atom twofold coordinated, which moves slightly off to the nanotube surface. We also find metastable configurations for (6,6) + 1 V and (10,0) + 1 V, 10.5 and 12.1 meV/atom higher in energy than their respective ground state (GS) geometries. In these configurations the pentagon structure plus the twofold coordinated C atom are also found but rotated about 60° with respect to the equilibrium geometries. A third metastable structure is found for (10,0) + 1 V, which is 17.2 meV/atom higher in energy than the GS geometry. Here, the C atoms adjacent to the vacancy do not form bonds, remaining twofold coordinated. This geometry is known as 3db (three dangling bonds) structure. Similar results for the GS and metastable geometries are found for the vacancy in the 11 Å diameter CNTs (8,8) and (14,0). The metastable geometries of (8,8) + 1 V and (14,0) + 1 V are 7.3 and 6.7 meV/atom higher in energy that the respective GS geometries. It is interesting to note that the 3db metastable structure of (10,0) + 1 V is not found in (14,0) + 1 V, suggesting that the 3db geometry exits due to the higher strain in the (10,0) tube, hindering further relaxations.

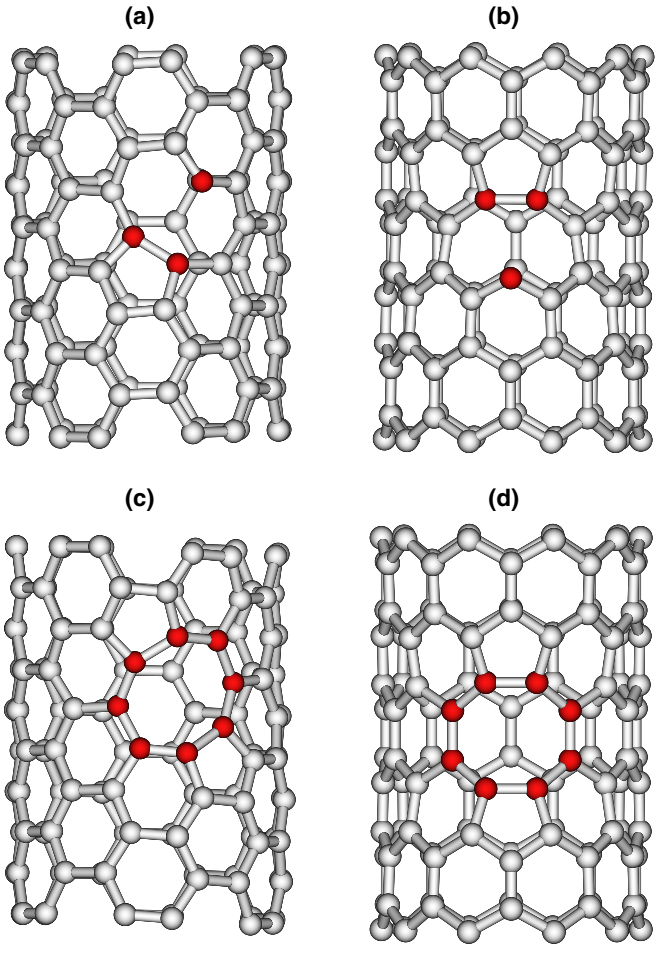

Fig. 1. Equilibrium geometry of the monovacancy and the divacancy in (6,6) and (10,0) CNTs. (a) (6,6) + 1 V, (b) (10,0) + 1 V, (c) (6,6) + 2 V, (d) (10,0) + 2 V. Red balls display the C atoms around the defect. (For interpretation of the references in color in this figure legend, the reader is referred to the web version of this article.)

The vacancy formation energies were calculated by

$$E_{\text{form}}(V) = E_{\text{tot}}(\text{CNT} + V) - E_{\text{tot}}(\text{CNT}) + \mu_{\text{C}} \quad (1)$$

where $E_{\text{tot}}(\text{CNT} + \text{V})$ and $E_{\text{tot}}(\text{CNT})$ are the total energy of the tube containing the vacancy and the perfect tube, respectively. μ_{C} is the carbon chemical potential which is calculated as the total energy per atom in the perfect tube. Our results are listed in Table 1 where we also include vacancy calculations performed in (6,6) and (10,0) CNTs considering a supercell with twice the length of the one previously used. We find that the vacancies in the 8 Å diameter CNTs have similar formation energies, ranging from 5.65 to 5.85 eV, including the longer supercell, whereas for the 11 Å diameter CNTs the formation energies tend to decrease due to the larger curvature.

Table 1 shows our results for the magnetic moment per defect site given by $m = 2\,S\mu_{\text{B}}$, where S is the spin and μ_{B} the Bohr magneton. We find that all nanotubes under con-

Table 1
Formation energy (E_{form}) and magnetic moment per defect (m) for the monovacancy and the divacancy in armchair and zigzag CNTs, considering different supercell lengths (L) or vacancy concentrations. $d_{\text{C–C}}$ is the equilibrium distance between C atoms that approach each other to form the pentagon bonding structure. In parenthesis are shown our results for the metastable geometries

System	L (Å)	m (μ_{B})	E_{form} (eV)	$d_{\text{C–C}}$ (Å)
(6,6) + 1 V	12.46	0.82 (1.1)	5.75 (7.00)	1.56 (1.93)
(6,6) + 1 V	24.92	0.63	5.85	1.57
(10,0) + 1 V	12.96	0.32 (1.0)	5.67 (7.11)	1.54 (1.72)
(10,0) + 1 V	25.92	0.49	5.65	1.53
(8,8) + 1 V	12.46	0.77 (1.1)	4.65 (5.81)	1.58 (1.98)
(14,0) + 1 V	12.96	0.53 (1.1)	5.20 (6.32)	1.58 (1.74)
(6,6) + 2 V	12.46	0.0 (0.0)	4.24 (7.84)	1.53 (1.78)
(6,6) + 2 V	24.92	0.0	4.17	1.52
(10,0) + 2 V	12.96	0.0 (0.0)	3.90 (6.65)	1.50 (1.65)
(10,0) + 2 V	25.92	0.0	4.06	1.49
(8,8) + 2 V	12.46	0.0	2.09	1.53
(14,0) + 2 V	12.96	0.0	2.33	1.50

sideration exhibit ferromagnetic ordering. The lower-energy structures of $(6,6)+1$ V and $(10,0)+1$ V have magnetic moments of 0.82 and 0.32 μ_B, respectively, whereas for the metastable configuration the magnetic moments are closer to 1 μ_B. Clearly, the magnetism is due to the under-coordinated C atom which has a localized unpaired spin, as shown in Fig. 2. As a C atom with a dangling bond has a magnetic moment of 1 μ_B, the lower magnetic moments found in $(6,6)+1$ V and $(10,0)+1$ V are due to a redistribution of charge around the defect. This can be checked by looking at the equilibrium distance between the C atoms that form the pentagon structure, shown in Table 1. As longer this distance is, larger is the magnetic moment. This means that once a vacancy is created, two of the three dangling bonds containing a spin rehybridize forming the pentagon structure. The weakness of this bond depends on the curvature strain of the tube. An extreme case occurs in the 3db configuration of $(10,0)+1$ V. Here no bond between the undercoordinated C atoms is formed, resulting in three dangling bonds with a total magnetic moment of 1.4 μ_B. Considering lower concentration of vacancies, that is doubling the supercell length, we find that magnetic moments on $(6,6)+1$ V and $(10,0)+1$ V change to 0.63 and 0.49 μ_B, respectively. The same behavior is observed for the tubes with higher diameters where the magnetic moment on $(8,8)+1$ V and $(14,0)+1$ V are 0.77 and 0.53 μ_B, respectively. The above results suggests that the magnetic moment would change with the distance between defects in CNTs. We are performing additional calculations to clarify this.

Fig. 3(b) and (c) shows the spin-resolved density of states (DOS) for $(6,6)+1$ V calculated with supercell lengths of L_1 and $2L_1$, which are compared with the perfect $(6,6)$ CNT (Fig. 3(a)). We observe that the $(6,6)$ armchair CNT preserves its metallic character for different vacancy

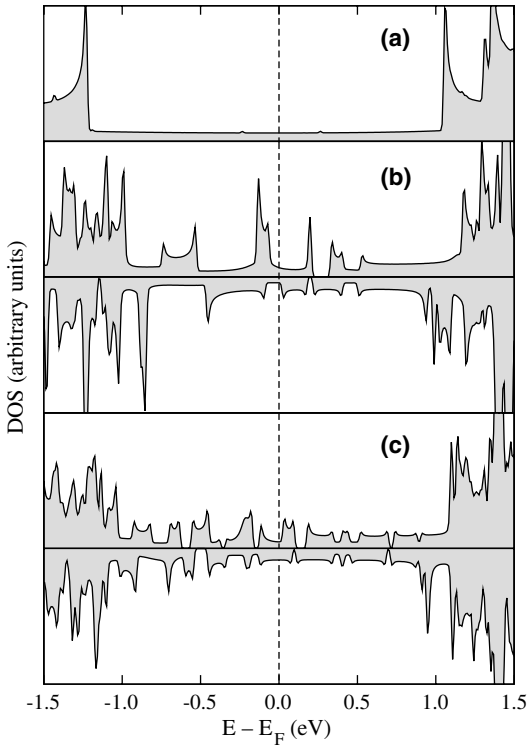

Fig. 3. Spin-resolved density of states (DOS) for the (6,6) CNT with a monovacancy. (a) The perfect (6,6) CNT, (b) $(6,6)+1$ V calculated with a supercell length of L_1 and (c) $(6,6)+1$ V calculated with a supercell length of $2L_1$. In (b) and (c), upper and lower panels correspond to majority and minority spin configurations, respectively. Dashed lines indicate the position of the Fermi level (E_F).

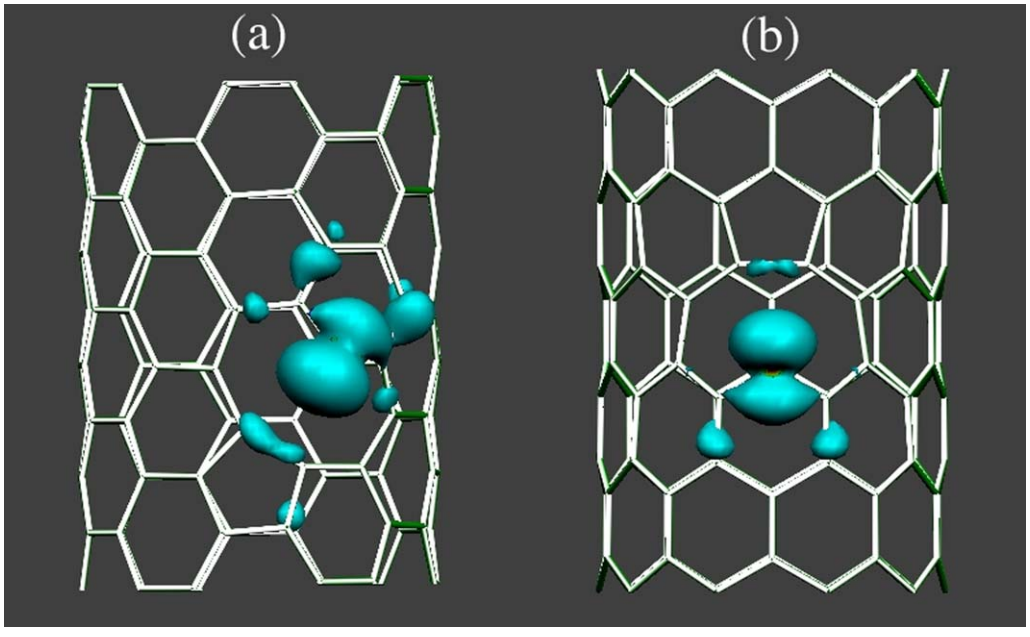

Fig. 2. Spin-density isosurfaces for the monovacancy in 8 Å diameter CNTs. (a) $(6,6)+1$ V and (b) $(10,0)+1$ V. The isosurfaces correspond to a charge of 0.015 e/Å^3.

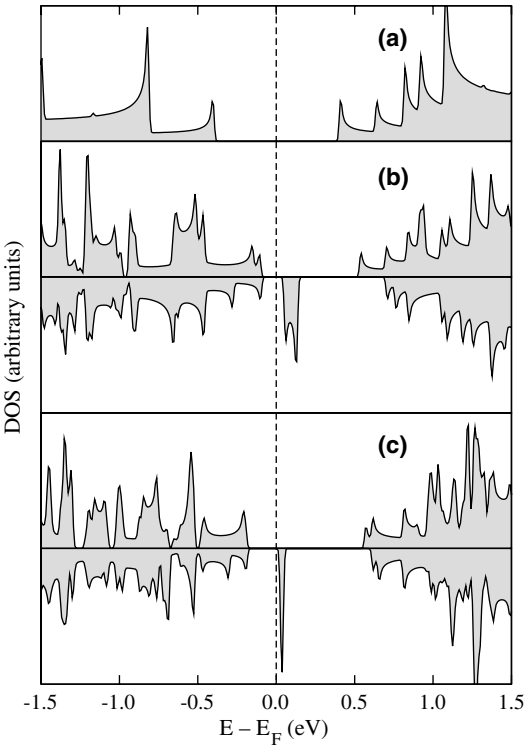

Fig. 4. Spin-resolved density of states for the (10,0) CNT with a monovacancy. (a) The perfect (10,0) CNT, (b) (10,0) + 1 V calculated with a supercell length of L_2 and (c) (10,0) + 1 V calculated with a supercell length of $2L_2$.

concentrations. We also note that the difference between majority (upper panel) and minority (lower panel) spin configurations in Fig. 3(b) and (c) clearly demonstrates the magnetism in the (6,6) + 1V system. Similar results are found for (8,8) + 1 V CNT which suggests that these properties would be also found in armchair CNTs with larger diameters. Fig. 4(b) and (c) shows the spin-resolved DOS for (10,0) + 1 V calculated with supercell lengths of L_2 and $2L_2$, which are compared with the perfect (10,0) CNT (Fig. 4(a)). As we can see, the (10,0) semiconducting CNT maintains this property when a C atoms is removed. For higher vacancy concentration the gap energy is about 0.1 eV mainly due to a defect state rising above the Fermi level. This state is localized at the uncoordinated C atom and at the C–C bond that form the pentagon. For lower vacancy concentration the defect state is less dispersive increasing the gap energy up to 0.2 eV.

4. The divacancy in carbon nanotubes

Fig. 1(c) and (d) displays the GS geometries for the divacancy in (6,6) and (10,0) CNTs (hereafter referred to as (6,6) + 2 V and (10,0) + 2 V). We find metastable geometries for (6,6) + 2 V and (10,0) + 2 V, which are 10.5 and 23.3 meV/atom higher in energy than the respective GS geometries. We observe that once a divacancy is created, the undercoordinated C atoms spontaneously reconstruct around the defect forming an octagon with two adjacent pentagons in opposite directions. For (6,6) + 2 V the pentagons point along a line of about 30° with respect to the tube axis, whereas in the metastable structure the pentagons are aligned normal to the tube axis. For (10,0) + 2 V the pentagons align along the tube axis for the GS geometry and along a line of about 60° with respect the tube axis. Similar equilibrium geometries for (8,8) + 2 V and (14,0) + 2 V were found, suggesting that these reconstructions should be also found in larger diameters CNTs. For the 8 Å (6,6) and (10,0) CNTs the divacancy formation energies are found to be 4.2 and 4.0 eV, respectively. For the 11 Å (8,8) and (14,0) CNTs the formation energies decrease to 2.1 and 2.3 eV, respectively, about half the value found in the 8 Å CNTs. This suggests that the curvature strain becomes important for the divacancy formation in small diameter CNTs. In Table 1 we also show the bond lengths between the C atoms that form the pentagon structure. The smaller bond length, of about 1.5 Å, are found for the divacancy in the zigzag (10,0) and (14,0) CNTs. As a consequence of the full reconstruction of the divacancy all C atoms around the octagon are threefold coordinated. Thus, no unpaired σ electron is found, implying that carbon nanotubes with this defect do not exhibit magnetism. Therefore, we can infer that the origin of the magnetism in nanotubes and graphite are mainly due to unpaired σ electrons which are localized. On the other hand, the delocalized π electrons would have a negligible contribution because once an unpaired σ electron reconstructs the magnetization disappear as shown by our divacancy results.

Fig. 5(b) and (c) shows the DOS for the (6,6) + 2 V system calculated with supercell lengths of L_1 and $2L_1$, respectively, which are compared with the perfect (6,6) CNT

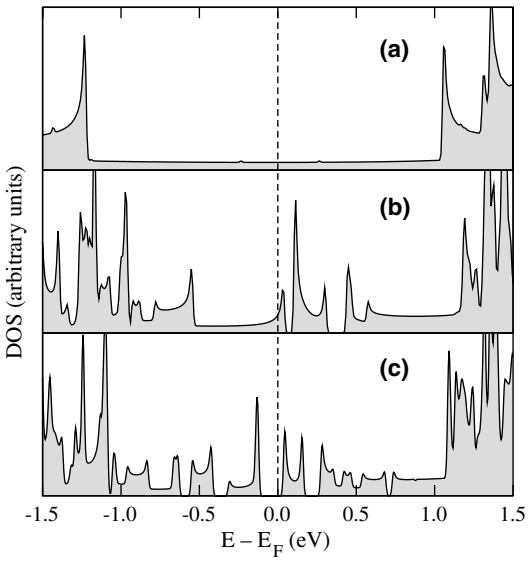

Fig. 5. Density of states for the (6,6) CNT with a divacancy. (a) Perfect (6,6) CNT, (b) (6,6) + 2 V calculated with a supercell length of L_1 and (c) (6,6) + 2 V calculated with a supercell length of $2L_1$.

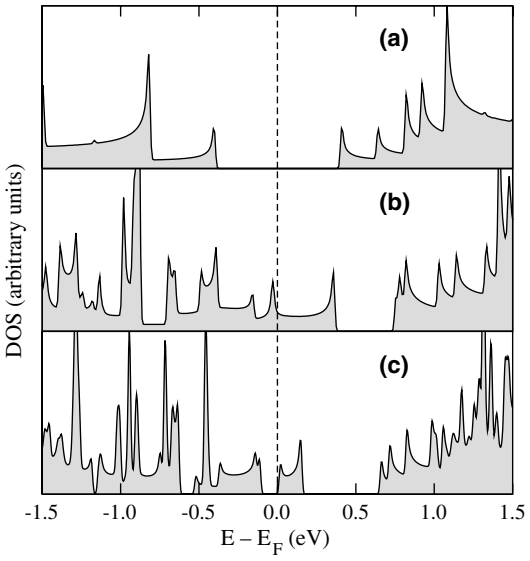

Fig. 6. Density of states for the (10,0) CNT with a divacancy. (a) Perfect (10,0) CNT, (b) (10,0) + 2 V calculated with a supercell length of L_2 and (c) (10,0) + 2 V calculated with a supercell length of $2L_2$.

(Fig. 5(a)). We find that for the higher defect concentrations, the system has a metallic character which is due to a CNT state that crosses the Fermi level at about 0.8ΓX. However, for the lower defect concentrations, the system becomes a semiconductor opening an energy gap of about 0.15 eV (Fig. 5(c)), which is due to the flattening of the defect state above the Fermi energy. Similar results are found for the (10,0) + 2 V system shown in Fig. 6. Here, the perfect (10,0) CNT is a semiconductor with an energy gap of 0.8 eV (Fig. 6(a)). For the higher defect concentrations, a defect state crosses the Fermi level at about 0.1ΓX, giving a metallic character to the system (Fig. 6(b)). For the more dilute defect concentrations, the (10,0) + 2 V system becomes semiconducting due to the flattening of the defect state (Fig. 6(c)). The defect states in both defective CNTs are localized at the atoms of the octagon. It is interesting to note that the (8,8) and (14,0) CNTs with a divacancy, calculated with supercell lengths of L_1 and L_2, respectively, also exhibit an energy gap of about 0.15 eV. This suggests that in CNTs with larger diameters, the energy gap should also increase due to the flattening of the defect state above to the Fermi energy.

5. Summary and conclusions

Based on ab initio calculations we have shown that CNTs with a monovacancy exhibit a ferromagnetic ordering induced by an undercoordinated C atom. The magnetic moment in the defect equilibrium geometries fluctuate among 0.3 and 0.8 μ_B, depending on the defect concentrations and on the CNT diameters. On the other hand, CNTs with a divacancy are not magnetic because all the C atoms around the defect are three-fold coordinated. The electronic structure shows that the monovacancy does not change the electronic character of the tubes. However, the divacancy can induce that both armchair and zigzag CNTs become small-gap semiconductors. The above properties suggest the possibility to achieve metal-free magnets and magnetic patterns at the nanometer scale.

Acknowledgements

We thank Millennium Nucleus of Applied Quantum Mechanics and Computational Chemistry for financial support, under project P02-004-F. W.O. also thanks FONDECYT for partially support this work under grant No. 1050197.

References

[1] T. Makarova, B. Sundqvist, P. Esquinazi, et al., Nature 413 (2001) 718.
[2] R.A. Wood, M.H. Lewis, M.R. Müller, D. Eckert, et al., J. Phys.: Condens. Matter 14 (2002) L385.
[3] P. Esquinazi, D. Spemann, R. Höhne, A. Setzer, K.-H. Han, T. Butz, Phys. Rev. Lett. 91 (2004) 227201.
[4] P.O. Lehtinen, A.S. Foster, Y. Ma, A.V. Krasheninnikov, R.M. Nieminen, Phys. Rev. Lett. 93 (2004) 187202.
[5] Y.-H. Kim, J. Choi, K.J. Chang, D. Tománek, Phys. Rev. B 68 (2002) 125420.
[6] M.S. Dresselhaus, G. Dresselhaus, Ph. Avouris, Carbon Nanotubes: Synthesis, Structure, Properties and Applications, Springer-Verlag, New York, 2001.
[7] Y. Ma, P.O. Lehtinen, A.S. Foster, R.M. Nieminen, New J. Phys. 6 (2004) 68.
[8] P. Ordejón, E. Artacho, J.M. Soler, Phys. Rev. B 53 (1996) R10441; J.M. Soler, E. Artacho, J.D. Gale, A. García, J. Junquera, P. Ordejón, D. Sánchez-Portal, J. Phys.: Condens. Matter 14 (2002) 2745.
[9] J.P. Perdew, K. Burke, M. Ernzerhof, Phys. Rev. Lett. 77 (1996) 3865.
[10] H.J. Monkhorst, J.D. Pack, Phys. Rev. B 13 (1976) 5188.